华侨大学
HUAQIAO UNIVERSITY

第五届桥梁抗震国际研讨会

The Fifth International Bridge Seismic Workshop (5IBSW)

GFRP- 钢双管约束橡胶混凝土组合墩柱抗震性能研究

SEISMIC PERFORMANCE OF GFRP-STEEL DOUBLE-SKIN CONFINED RUBBER CONCRETE COMPOSITE BRIDGE PIERS

Prof. Hai-feng Li (李海锋 教授)

College of Civil Engineering, Huaqiao University

Changsha, China

June 6, 2026

华侨大学 HUAQIAO UNIVERSITY

CONTENTS

1 Research Background

2 Axial compressive behavior

3 Seismic performance

4 Residual seismic performance

5 Conclusions and Outlook

1.1 Reinforced concrete (RC) bridge piers

Typical distresses include:

- Carbonation is widely observed in the concrete cover;
- The reinforcement in the bridge piers is exposed to water and suffers from corrosion-induced expansion;
- Subsequent strengthening and rehabilitation are challenging, maintenance costs are high, and numerous unforeseeable risks may arise.

Key issue 1：

Address the problem of environment-induced corrosion in RC piers

01. Research Background

1.2 Steel bridge piers

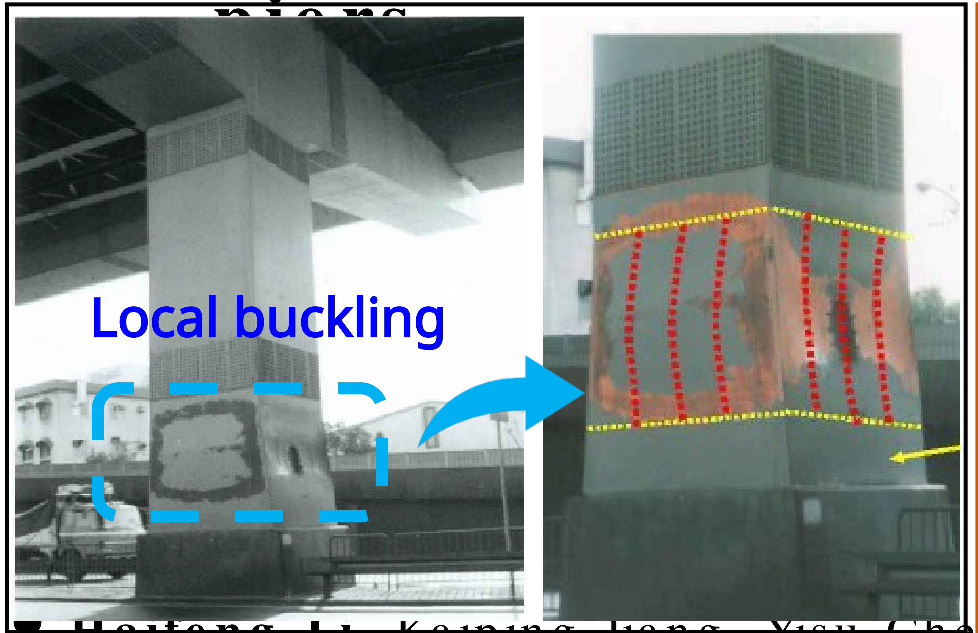

Key issue 2：

Address the problems of corrosion susceptibility and local buckling failure in steel piers.

- **Haifeng Li**, Kaiping Jiang, Yisu Chen, Xue Tian. Seismic behavior of steel tubular bridge columns equipped with low-yield-point steel plates in the root replaceable pier[J]. ***Earthquake Engineering and Engineering Vibration***, 2023, 22(2): 527-548.
- **Haifeng Li**, Kunde Lv, Runsheng Cui. Seismic behaviour of eccentrically compressed steel-box bridge-pier columns with embedded energy-dissipating shell plates[J]. ***Bulletin of Earthquake Engineering***, 2020, 18: 3401-3432.
- **Haifeng Li**, Yongfeng Luo. Experimental and Numerical Study on Cyclic Behavior of Eccentrically-

1.3 Rubber concrete

Waste tires (Solid waste)

Rubber particles

Rubber concrete

Characteristics

- ✓ Good elasticity, vibration reduction, and noise reduction;
- ✓ High deformability;
- ✓ Fatigue and aging resistance;
- ✓ Impact and crack resistance
- ✓ Good durability and toughness;
- ✓ Low strength.

Key issue 3: Overcome the limitations of insufficient strength in the engineering application of rubber concrete.

1.4 Novel composite materials

Issues

- To address the deterioration of RC piers induced by environmental exposure;
- To address the corrosion susceptibility and local buckling failure of steel piers;
- To overcome the limitations of insufficient strength on the engineering application of rubberized concrete.

FRP
GFRP
CFRP
et al.

Novel composite materials are considered ideal candidates for extending the service life of engineering structures because of their corrosion resistance, low weight, and high strength.

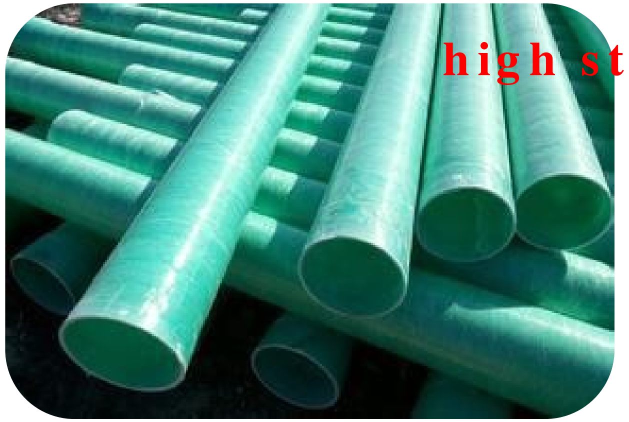

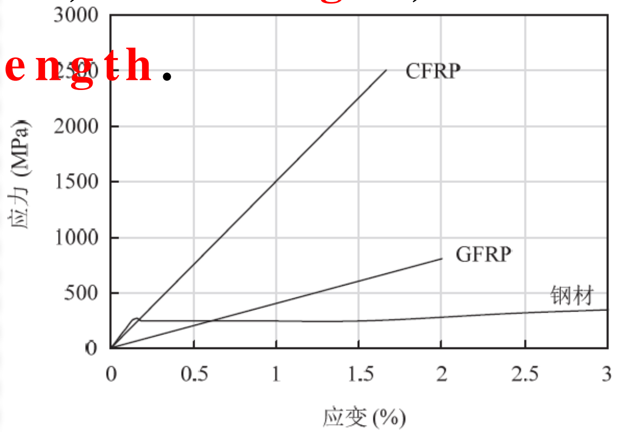

1.5 Design of composite bridge piers

Composite bridge piers = **GFRP tube** + **Rubber concrete** + **Hollow Steel tube**

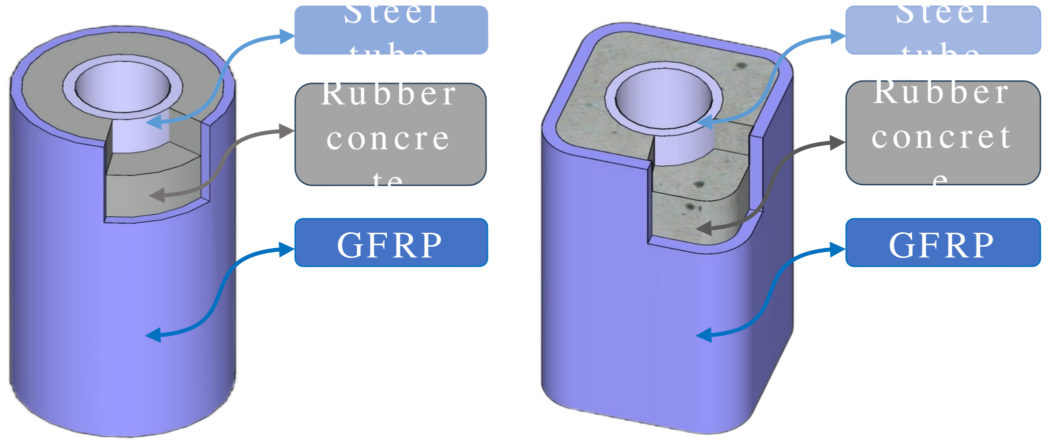

GFRP-steel double-skin confined rubber concrete composite bridge piers

- Enhanced load-bearing capacity, ductility, and durability;
- Improved mechanical properties of rubber concrete;
- Steel tubes replacing reinforcing bars to provide sufficient flexural resistance;
- Higher construction efficiency;
- Reduced carbon emissions.

CONTENTS

1 Research Background

2 **Axial compressive behavior**

3 Seismic performance

4 Residual seismic performance

5 Conclusions and Outlook

2.1 Tests and results analysis of square composite bridge piers

Construction

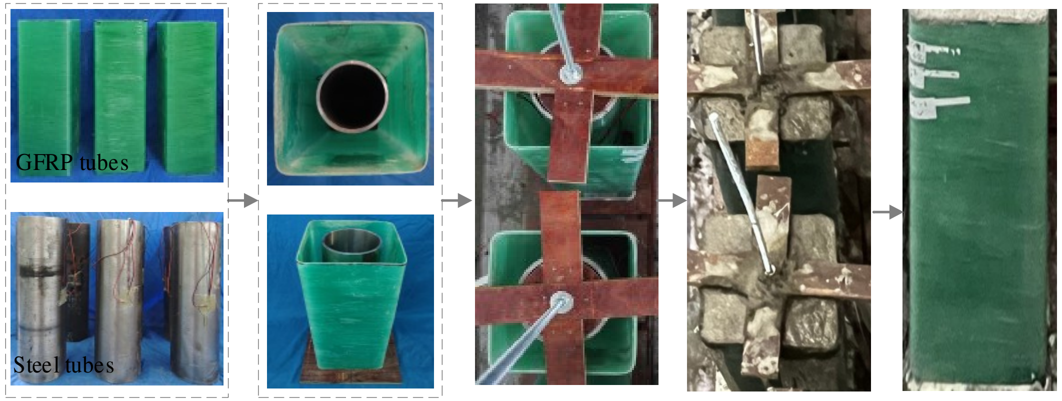

Failure modes

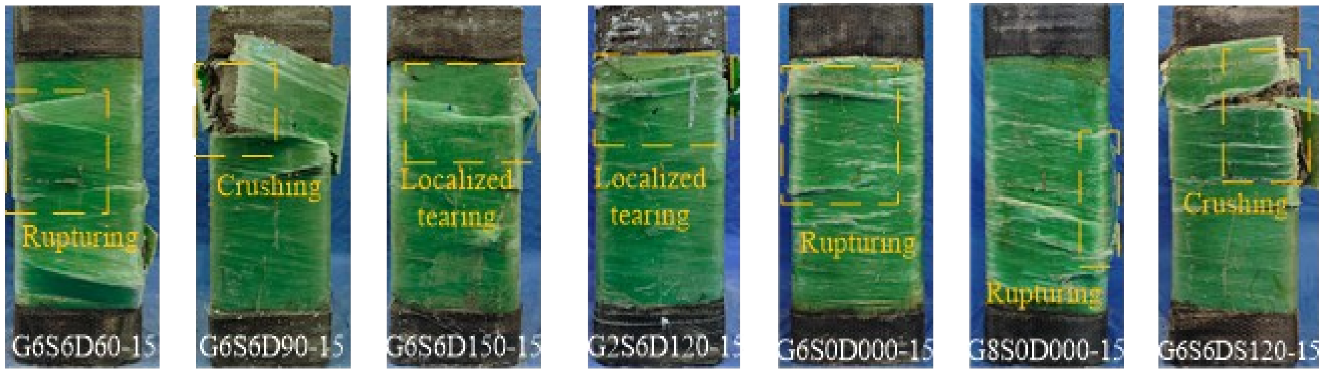

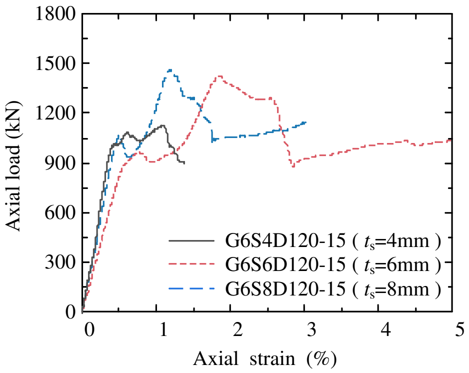

Steel tube thickness

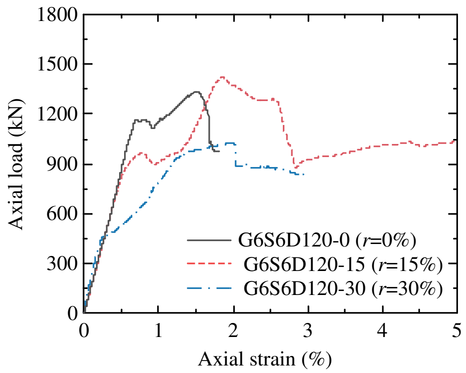

Rubber content

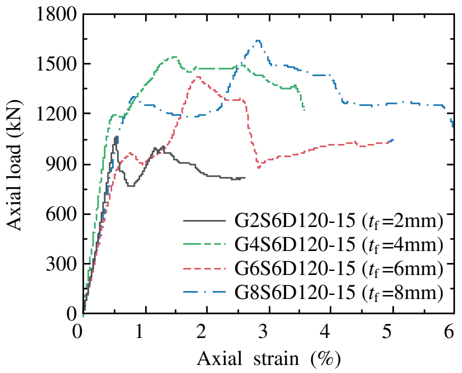

GFRP thickness

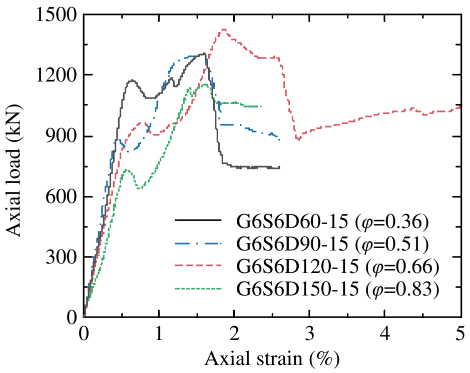

Void ratio

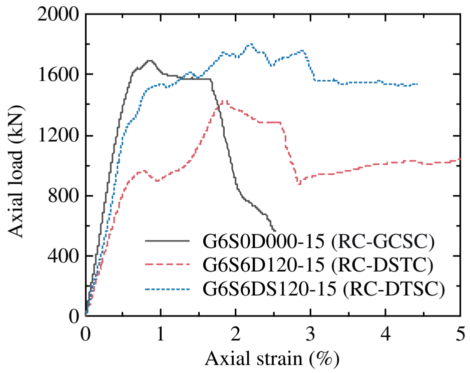

Cross-sectional shape

02. Axial compressive behavior

華僑大學 HUAQIAO UNIVERSITY

2.2 Parameter analysis and load-carrying capacity prediction of square composite bridge piers

Analysis of key

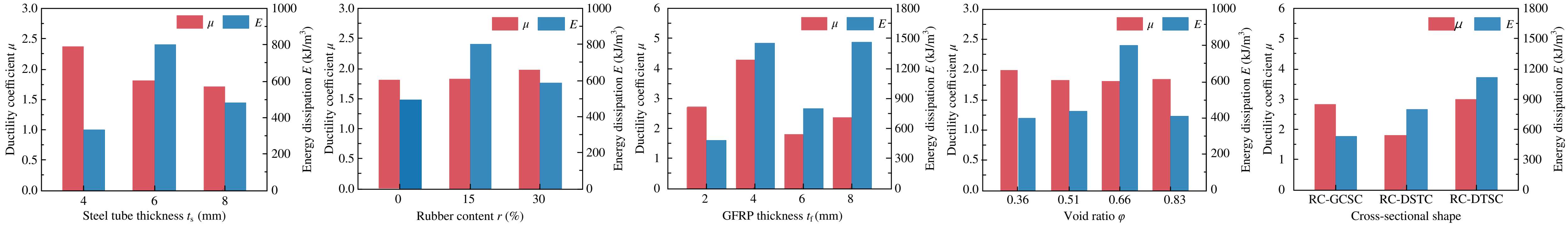

Calculation model for load-carrying

- Load-carrying capacity：[illegible]

(1) GFRP tube：

[illegible]

(2) Steel tube：

$$N_s = A_s\sigma_{s1} = A_s\left(\sqrt{f_y^{2} - \frac{3P_2^{2}D_0^{2}}{16t_s^{2}}} + \frac{P_2D_0}{4t_s}\right)$$

(3) Sandwich concrete：

$$N_c = A_c\left(f_{c0}k_r + kk_sk_ck_\varphi\left(P_1 + P_2\right)\right)$$

$$P_1 = [illegible]$$

$$P_2 = \frac{Vf_y}{\sqrt{\frac{3D_0^2}{16t_s^2}\left(\frac{3D_0^2}{16t_s^2} + V^2\right)}}$$

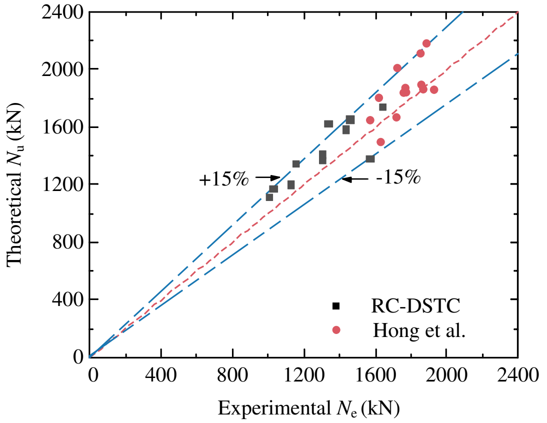

- Kaige Liu, **Haifeng Li**, Hanhuang Huang, et al. Axial compressive behavior and capacity calculation of GFRP-rubberized concrete-steel double-skin tubular square columns with large void ratios[J]. Structures, 2026. (Under Review)

02. Axial compressive behavior

HUAQIAO UNIVERSITY

2.3 Tests and analysis of elliptical composite bridge piers

Design and fabrication of

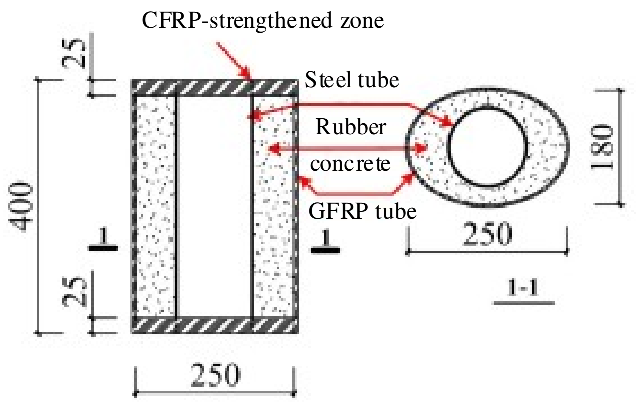

Finite element

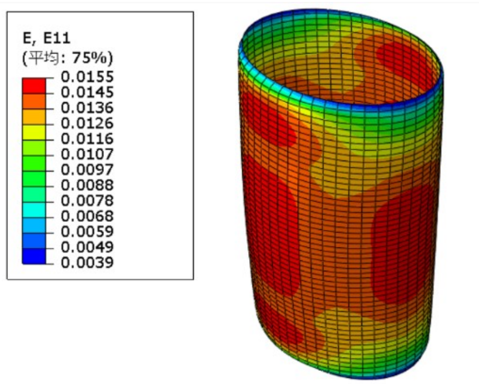

Load-displacement

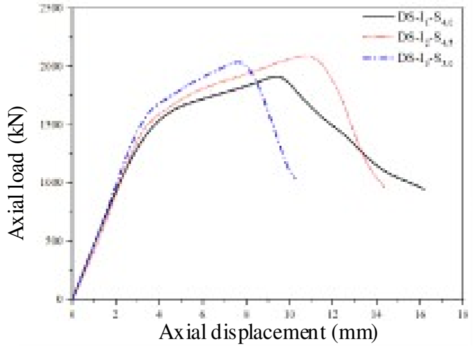

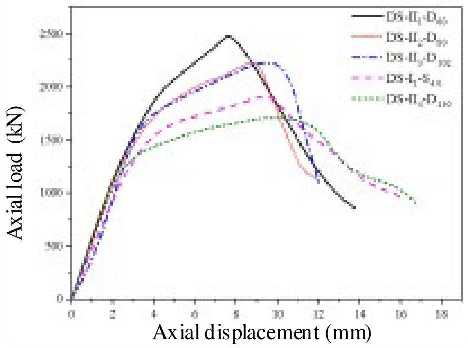

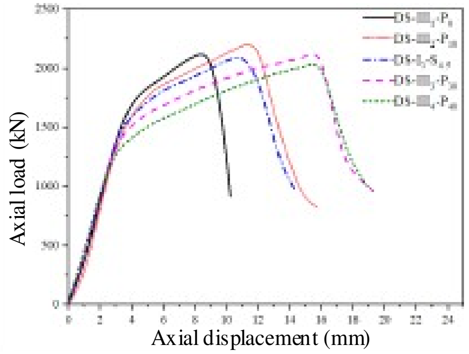

2.4 Parametric analysis of elliptical composite bridge piers

Steel tube

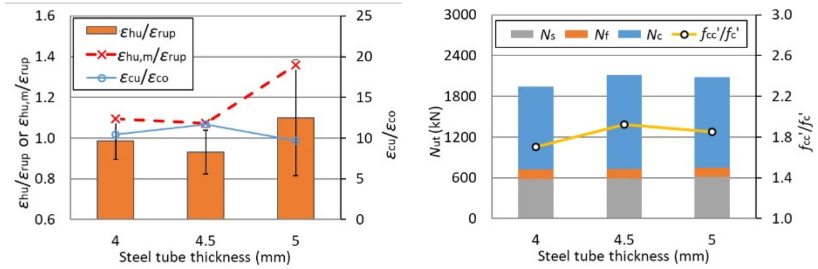

Hollow

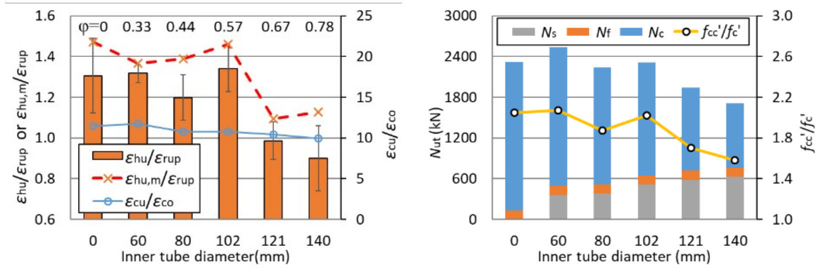

Rubber

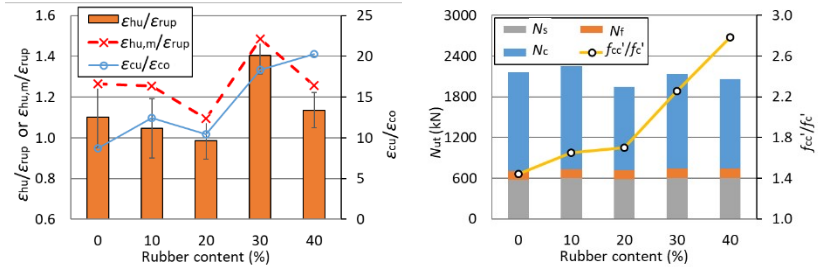

Rubber

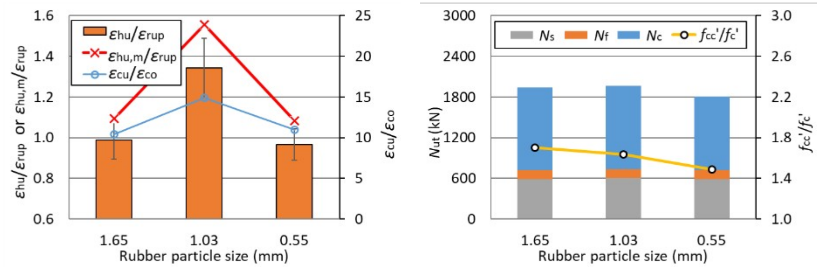

GFRP

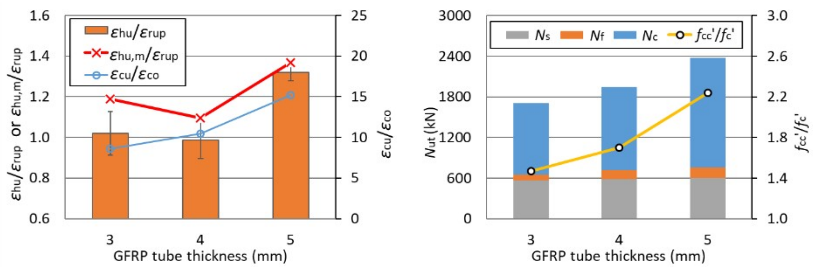

Rubber content (Solid

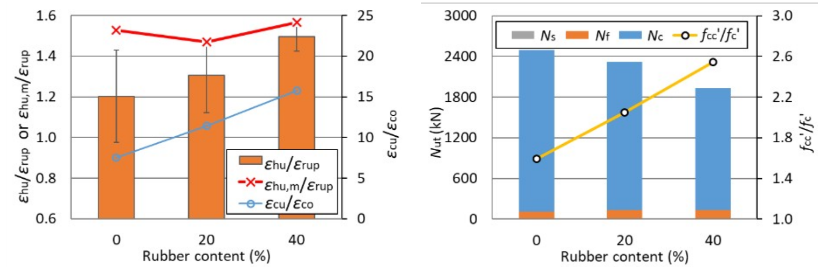

2.5 load-carrying capacity prediction of elliptical composite bridge piers

Hoop strain：

$$\varepsilon_{hu} = k_s k_\varphi \varepsilon_{f\ldots}$$ [illegible]

$$k_s = 0.5(3 - \frac{D_a}{D_b})$$

$$k_\varphi = \ldots$$ [illegible]

Axial strain：

$$D_e = \frac{D_a^2}{D_b}$$

$$f_l = \frac{2E_f t_f \varepsilon_{hp}}{D_e}$$

$$f'_{cc} = f'_c + k f_l$$ [illegible]

$$k = \ldots$$ [illegible]

$$\varepsilon_{cu} = \ldots \frac{f'_{cc}}{f'_c} - \ldots$$ [illegible]

Calculation model：

$$N_u = N_s + N_f + N_c$$ [illegible]

$$N_c = A_c f_{cc}$$ [illegible]

$$N_s = A_s f_{sy}$$

$$N_{ff} = \ldots$$ [illegible]

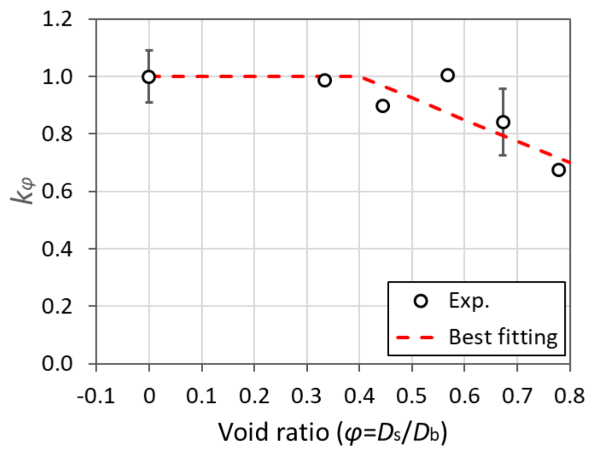

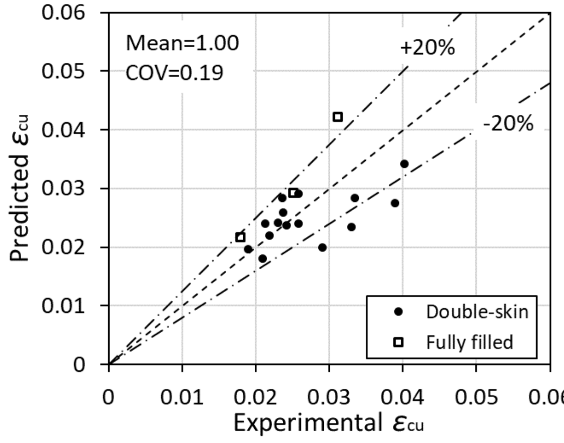

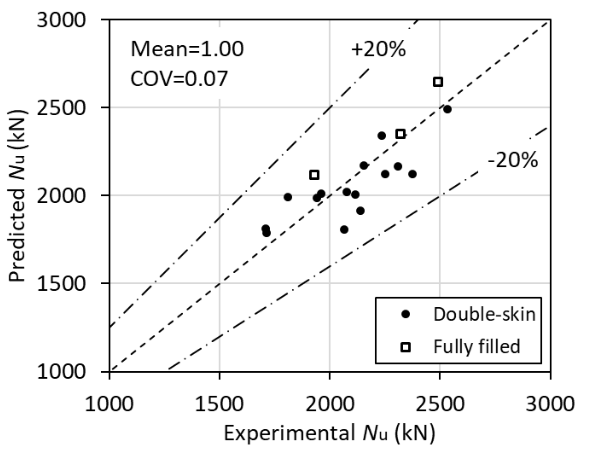

- **Haifeng Li**, Yinglei Li, Zhe Xiong, et al. Experimental and theoretical study on elliptical rubber concrete filled double-skin GFRP short tubes under axial compression[J]. ***Construction and Building Materials***, 2023, 401: 132796.

HUAQIAO UNIVERSITY

CONTEN TS

1 Research Background

2 Axial compressive behavior

3 **Seismic performance**

4 Residual seismic performance

5 Conclusions and Outlook

3.1 Test design of square composite bridge piers

A total of seven composite pier columns were designed with the **axial compression ratio**, **rubber content**, and **GFRP tube thickness** as the main test parameters.

Design parameters

Specimen ID	Axial compression ratio	Rubber content (%)	Thickness of GFRP tube (mm)	N (kN)
n0.1-ρ20-t5	**0.1**	20	5	185.15
n0.2-ρ20-t5	**0.2**	20	5	370.30
n0.3-ρ20-t5	**0.3**	20	5	555.45
n0.2-ρ10-t5	0.2	**10**	5	455.07
n0.2-ρ30-	0.2	**30**	5	324.55

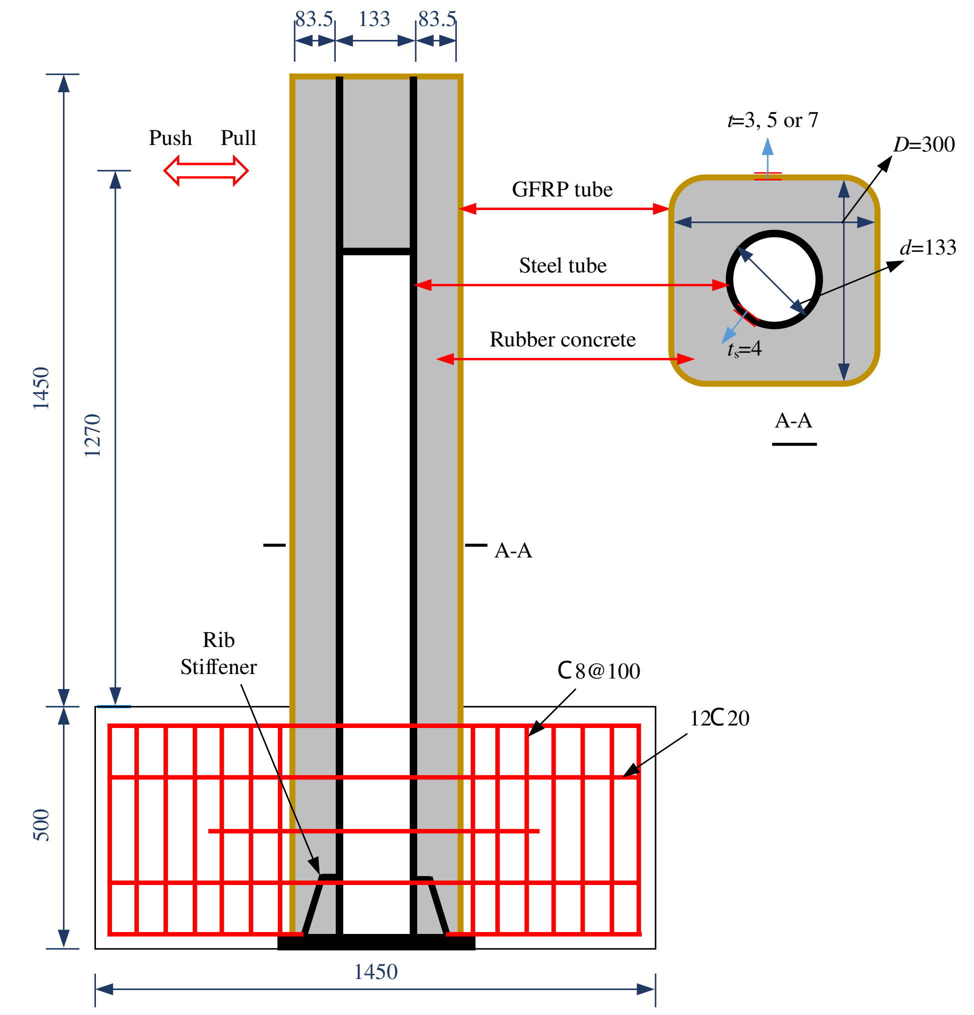

Configuration of the Specimen

3.2 Experimental program of square composite bridge piers

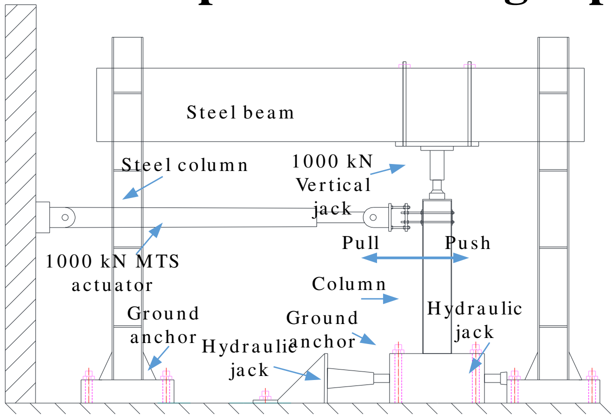

Schematic of the Loading Setup

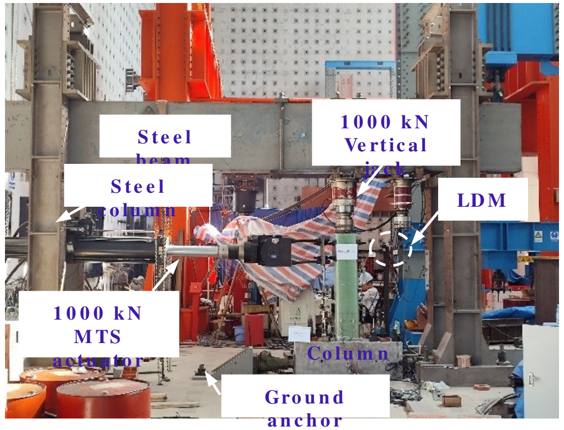

Loading scene

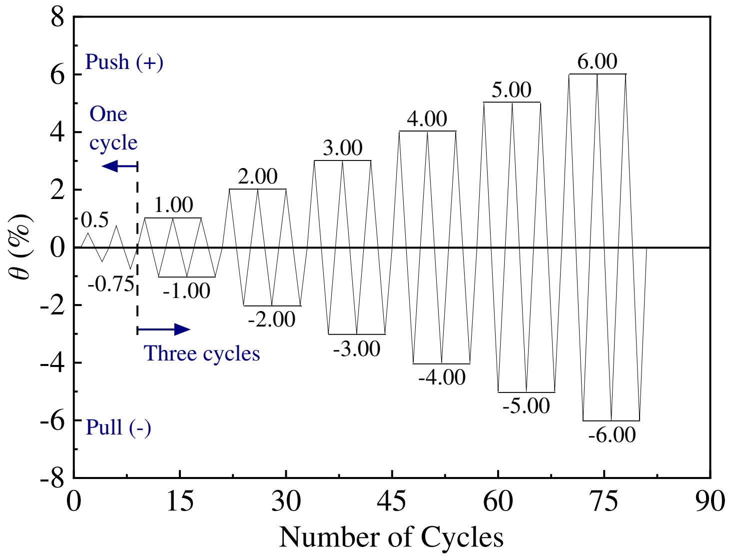

Loading protocol

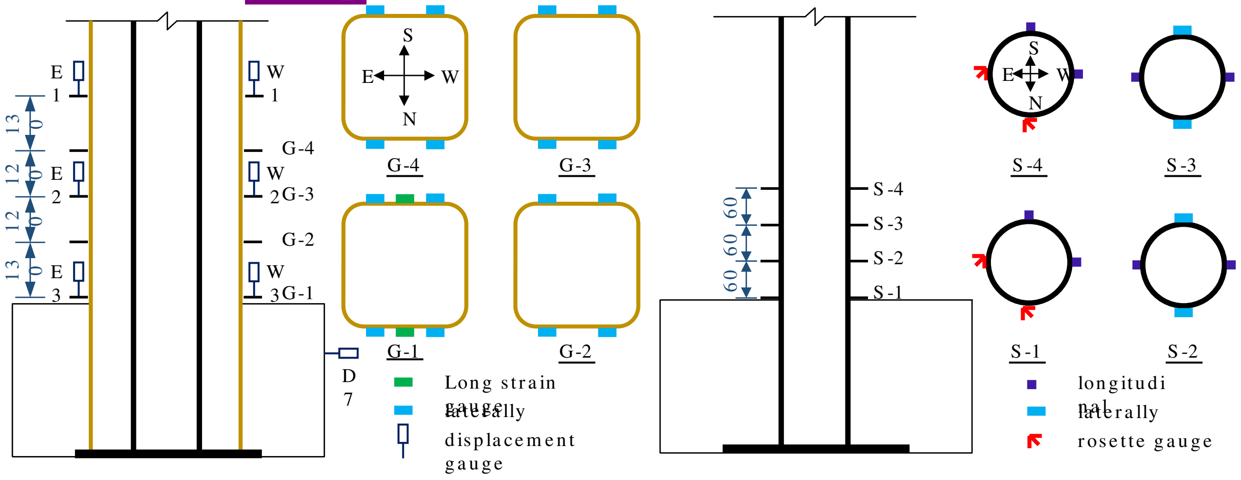

Measurement Scheme

When θ = 0.5% and 0.75%, one cycle was applied at each level; when θ = 1%, 2%, 3%, 4%, 5%, and 6%, three cycles were applied at each level, until the lateral load dropped to 85% of the peak load or obvious damage occurred and the specimen could no longer be loaded, at which point the specimen

3.3 Failure modes of square composite bridge piers

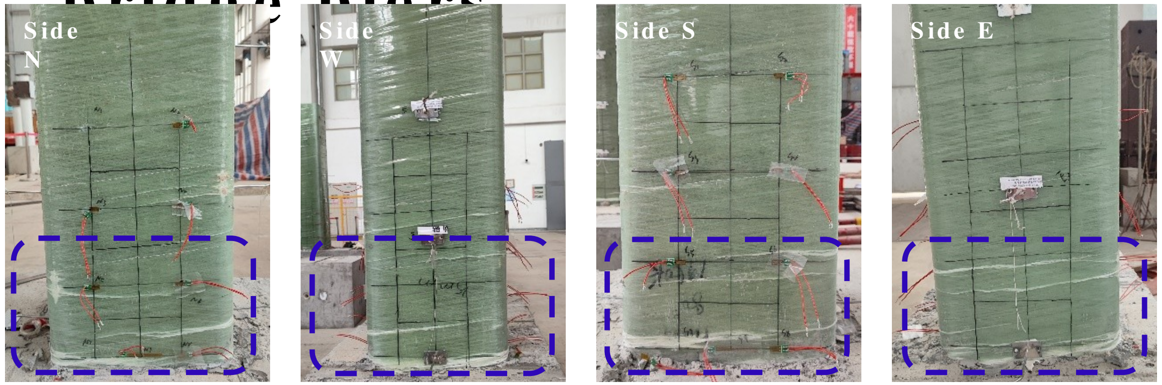

Failure modes of typical specimens

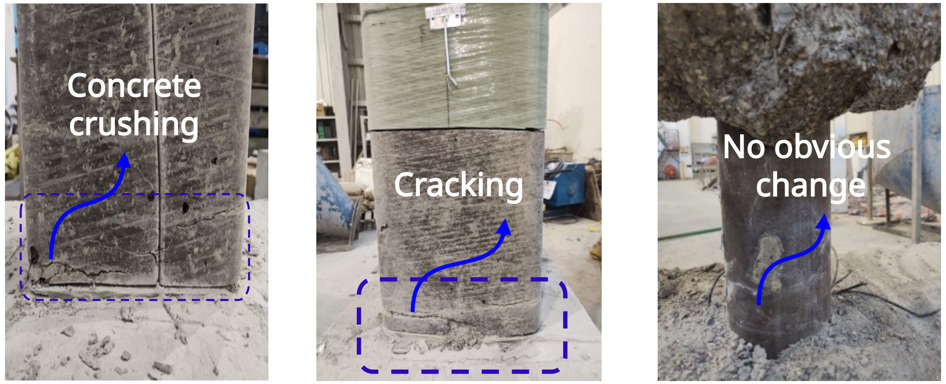

Failure modes of rubber concrete and steel tubes

- The composite pier columns exhibited similar failure modes, with **damage concentrated within 0-150 mm above the pile cap**.
- After the GFRP tube was removed, it could be seen that obvious **cracks appeared in the rubber concrete on the inner side corresponding to the damaged locations of the GFRP tube**, whereas no obvious cracking or other similar phenomena were observed on the surface of the rubber concrete corresponding to the undamaged locations of the GFRP tube.
- After the rubber concrete was removed, the surface of the hollow steel tube showed **no obvious buckling, cracking, or other damage, and remained in good condition**.

3.4 hysteresis behavior of square composite bridge piers

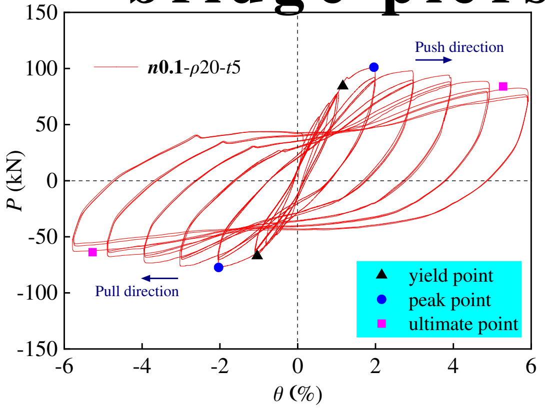

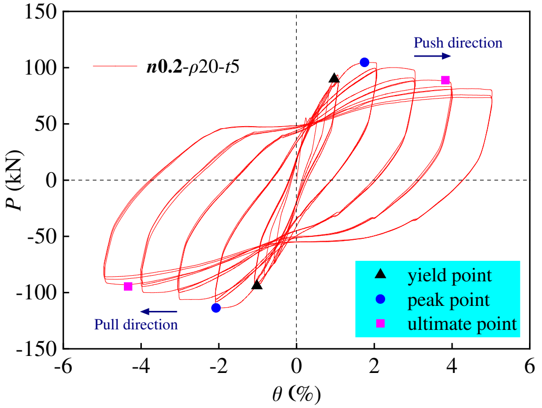

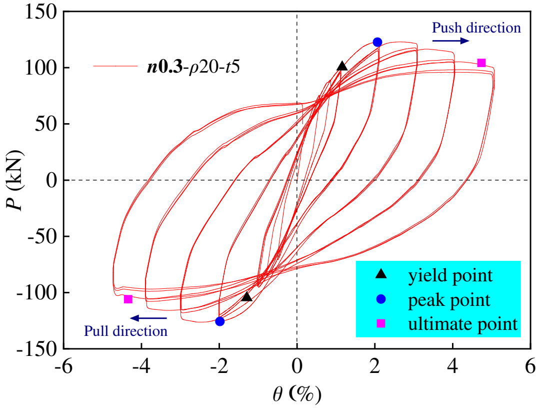

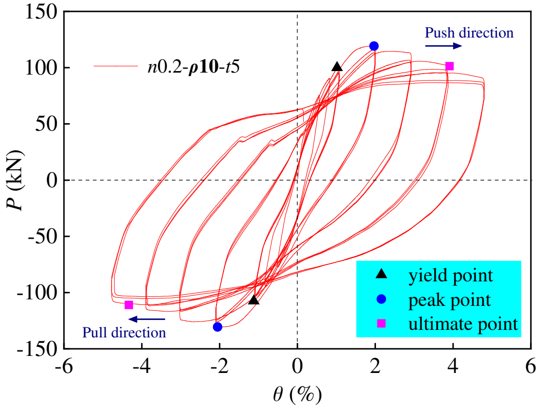

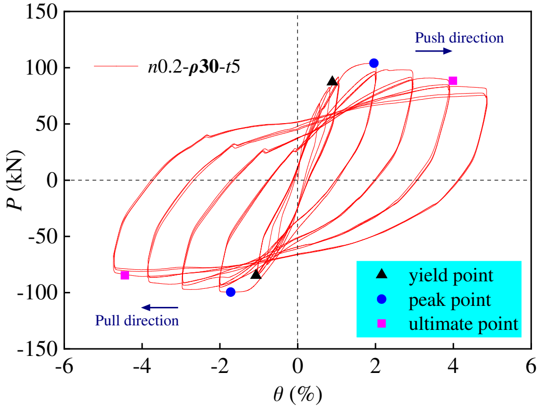

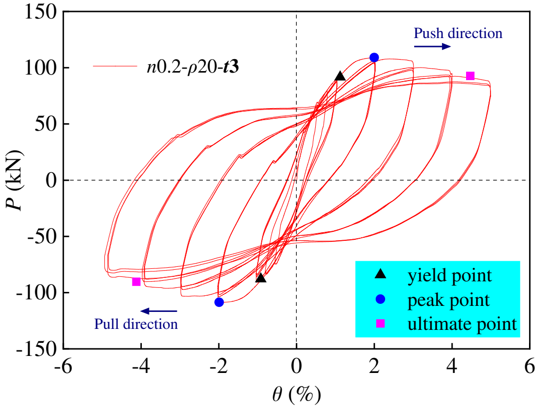

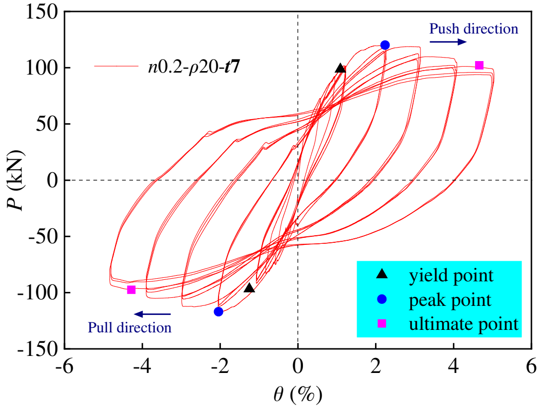

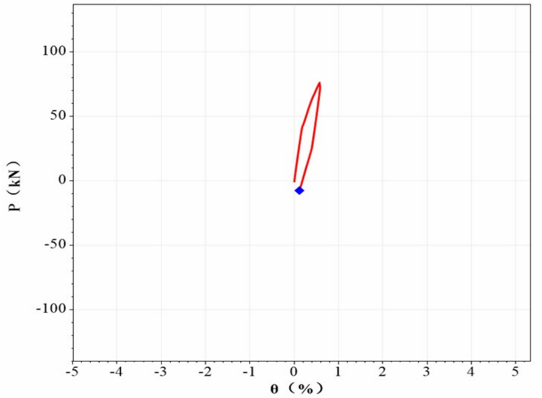

- Jianhuang Yan, Junchao Wu, Yang Xiang, Anlong Jiang, Hualin Cao, Xue Han, **Haifeng Li**. Seismic performance assessment of GFRP-steel double-skin confined rubber concrete composite columns[J]. ***Journal of Constructional Steel Research***, 2024, 216: 108597

3.5 Prediction of lateral capacity of square composite bridge piers

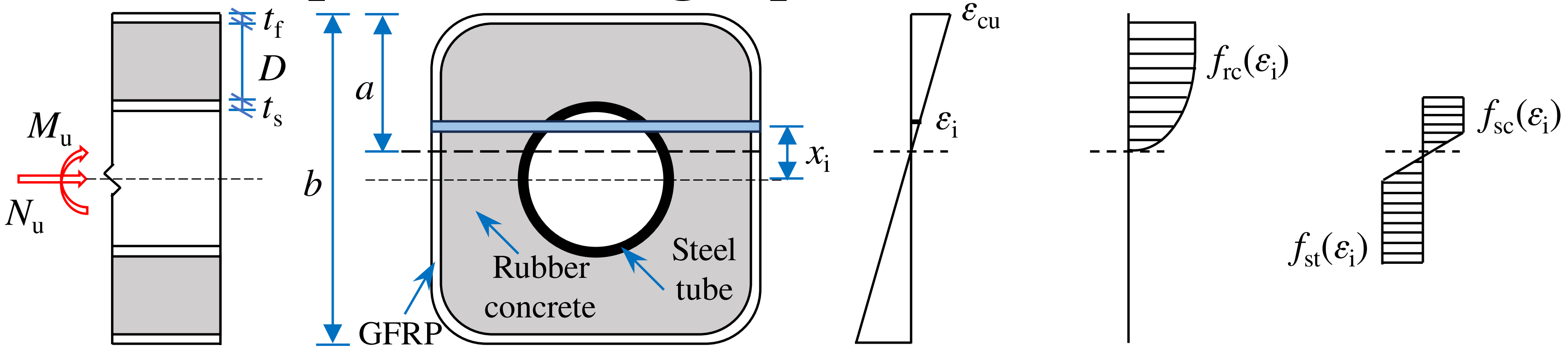

(a) Schematic diagram in cross-section (b) The compression area of the cross-section (c) Distribution of strain (d) Stress state of concrete (e) Stress state of steel tube

Prediction of lateral capacity of square composite bridge piers

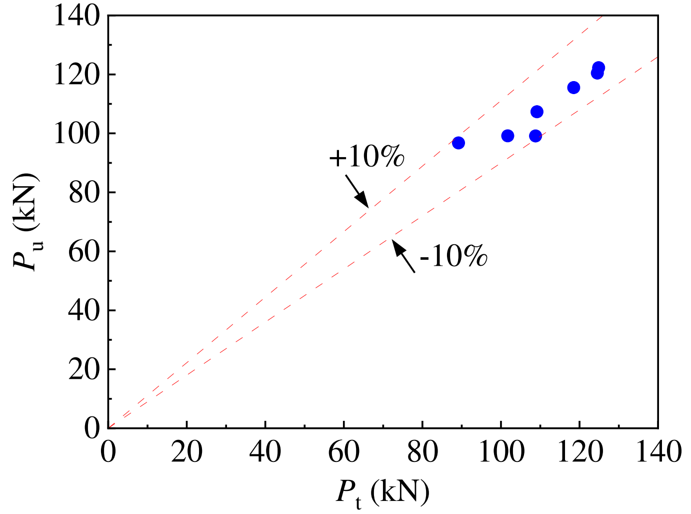

Comparison of predicted results

Sectional Strain at a Distance x_i from the Centroid：

$$\varepsilon_i = \frac{x_i-(b/2-a)}{a}$$

Capacity equation：

$$P_u = \frac{M_u}{l}$$

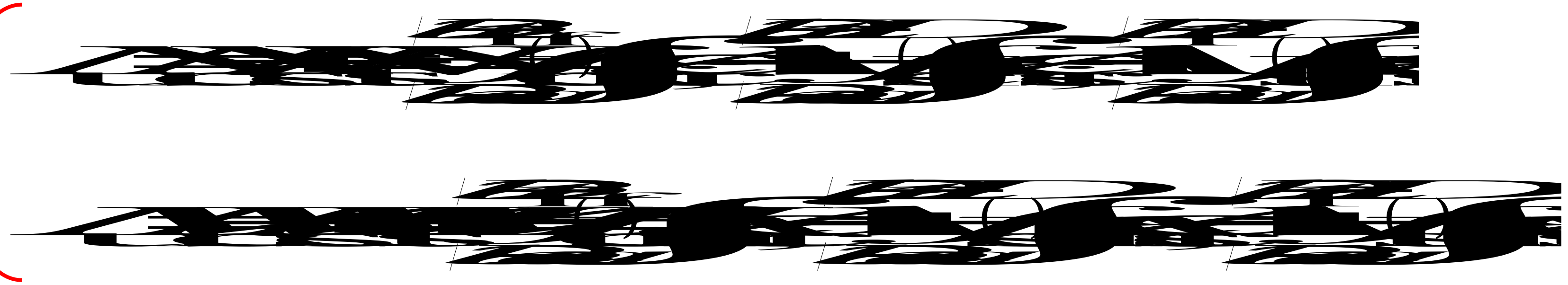

3.6 Tests and analysis of circular composite bridge piers

Design parameters

Specimes	R/%	D_1/mm	n	N_1/kN
R0-D180-N0.2	0	180	0.2	660
R20-D180-N0.2	20	180	0.2	590
R40-D180-N0.2	40	180	0.2	462
R20-D168-N0.2	20	168	0.2	566
R20-D159-N0.2	20	159	0.2	568
R20-D180-N0.1	20	180	0.1	295
R20-D180-N0.25	20	180	0.25	738

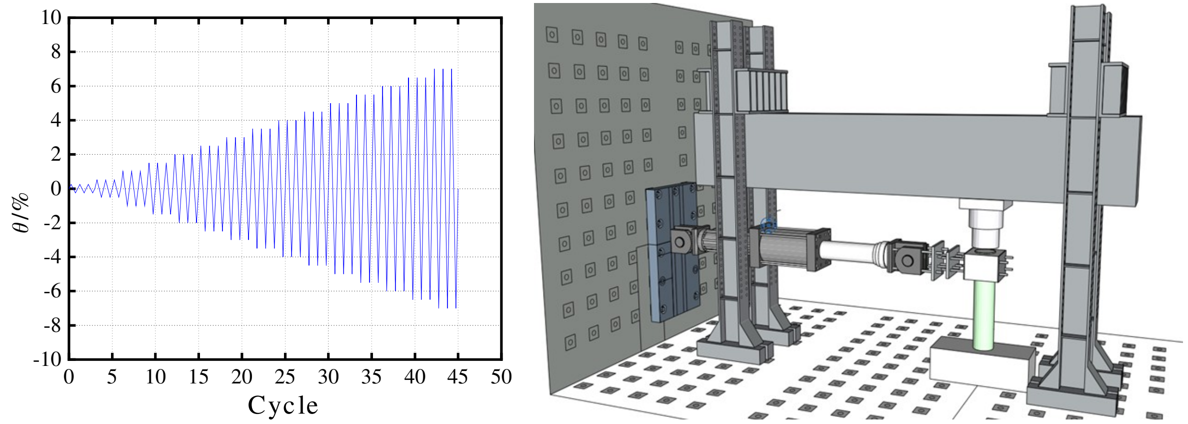

Loading protocol

Failure modes

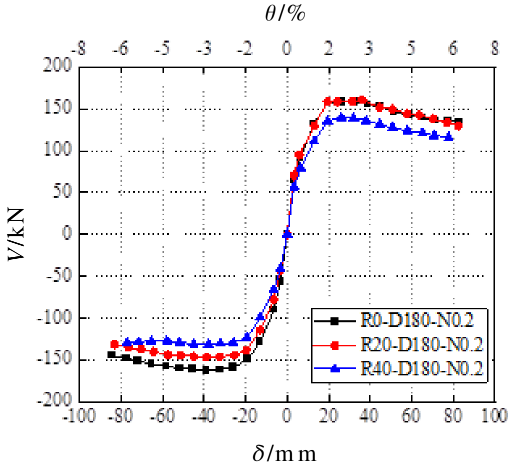

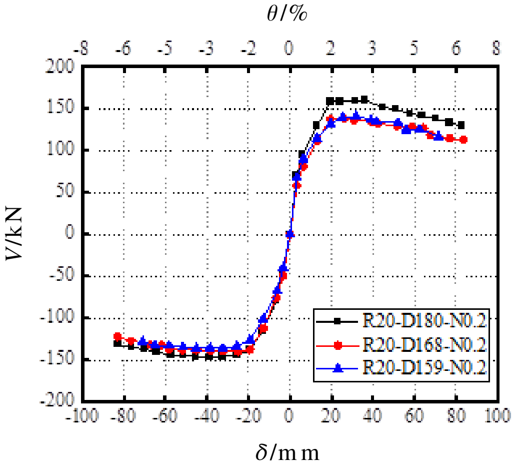

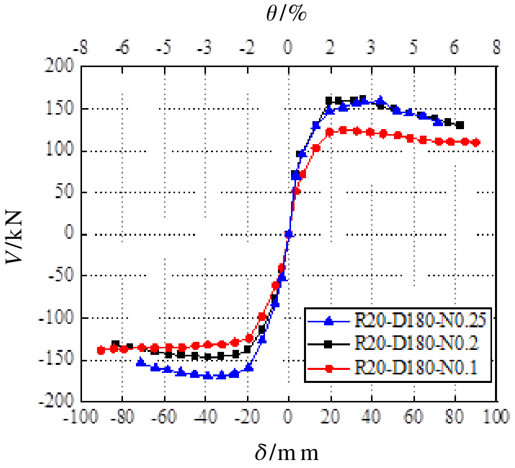

3.7 Development of a restoring force model for circular composite bridge piers

① Fixed-point：$V_d^+ = 0.7V_{max}^+ \quad V_d^- = 0.65V_{max}^-$

② End point of the descending branch： $V_z = 0.7V_f$

③ Unloading stiffness： $K_T = 0.6(\frac{K_0^- + K_0^+}{2})$

④ Softening point：

$$V_r^+ = (0.00006V_{max}^- + 0.01379)\delta^2 + 0.00693V_{max}^-\delta - 6.07593$$

$$V_r^- = (0.00007V_{max}^+ - 0.01260)\delta^2 - 0.00635V_{max}^+\delta + 22.24863$$

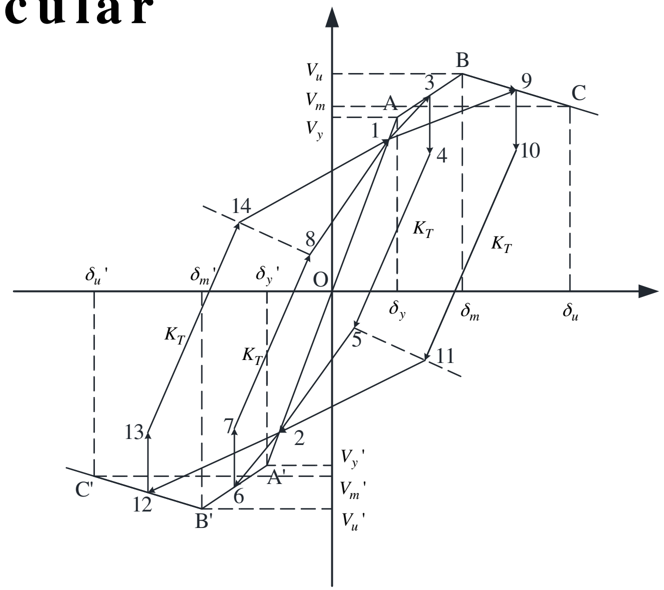

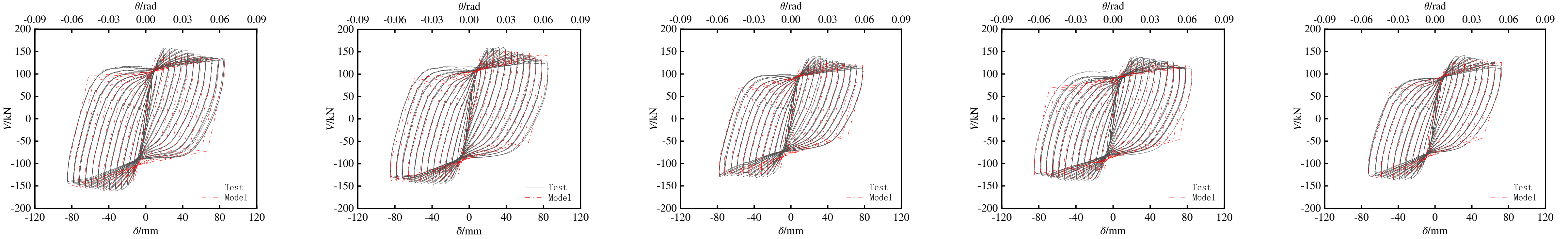

- Kaiping Jiang, Jingjie Yang, Xue Han, Ziqin Jiang, **Haifeng Li**. Seismic performance of GFRP-rubberized concrete-steel hybrid solid columns[J]. ***Structures***, 2023, 58: 105430.

CONTENTS

1 Research Background

2 Axial compressive behavior

3 Seismic performance

4 Residual seismic performance

5 Conclusions and Outlook

4.1 Design and manufacturing

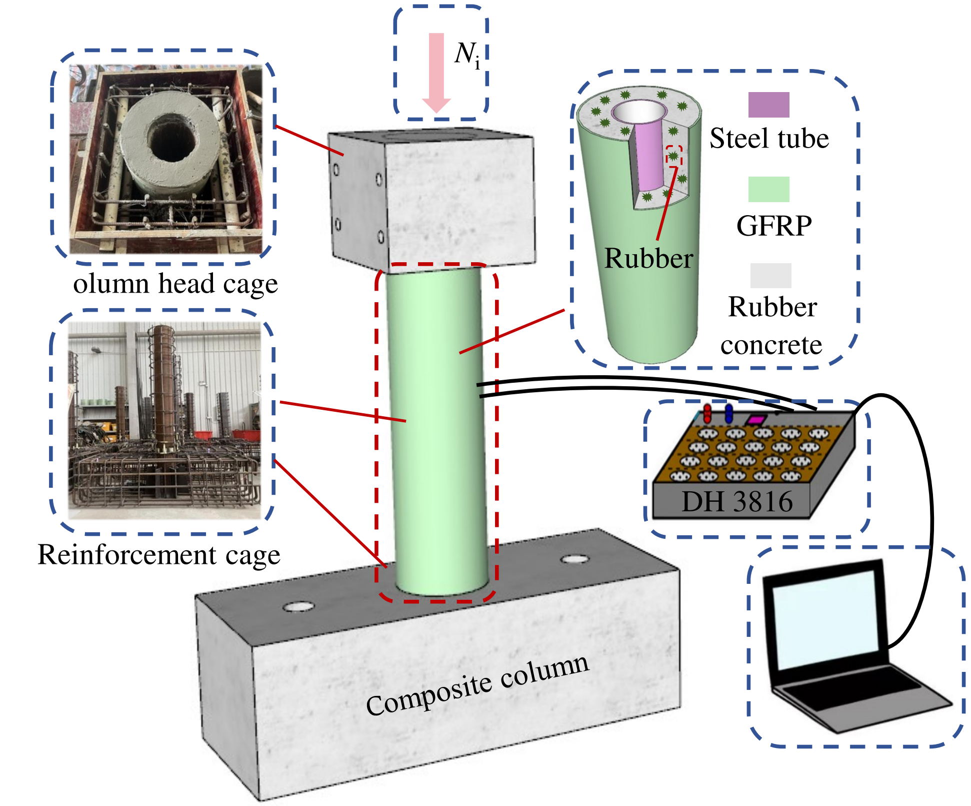

Configuration and fabrication of composite bridge piers

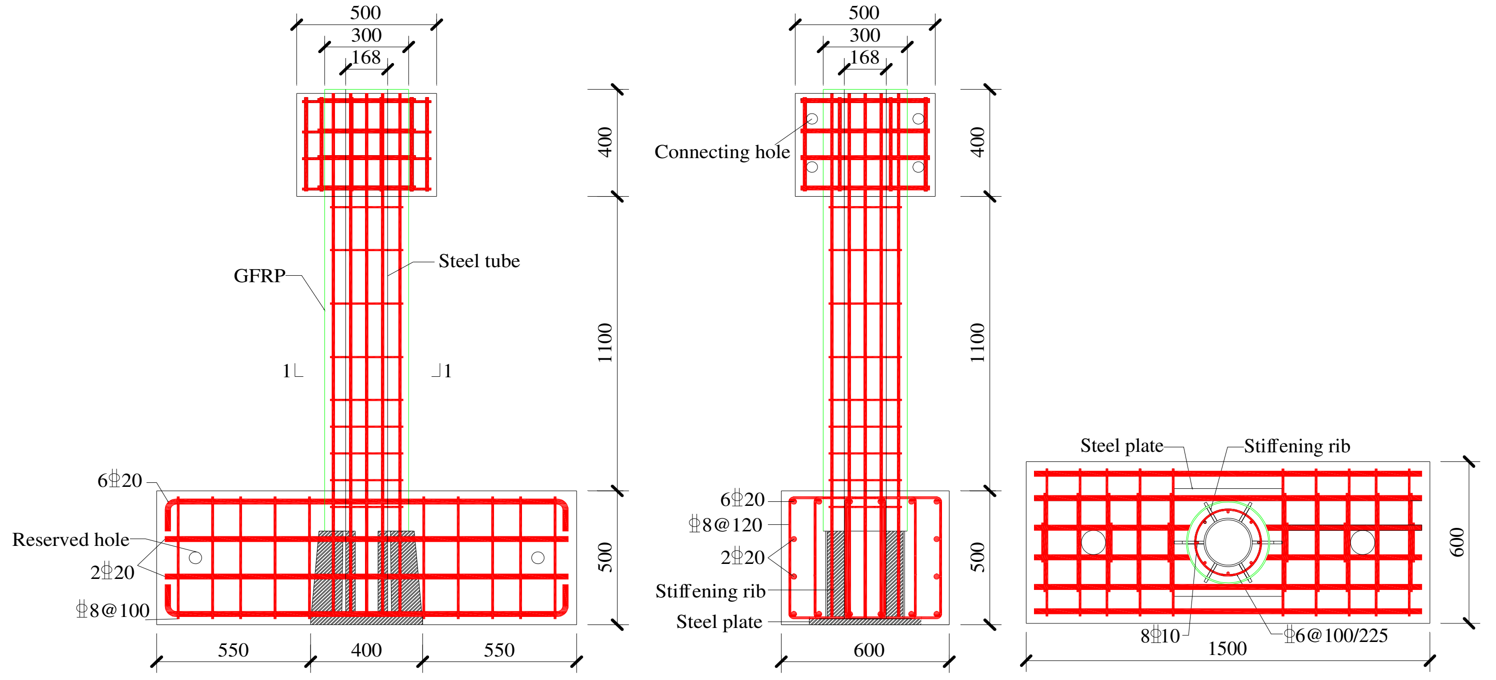

Reinforcement details and dimensions

Design parameters

Specimen	R (%)	D_1 (mm)	t_1 (mm)	D_2 (mm)	t_2 (mm)	n	N_i (kN)
R0N0.2	0	168	6	300	6	0.2	672
R15N0.2	15	168	6	300	6	0.2	401
R30N0.2	30	168	6	300	6	0.2	582
R15N0.1	15	168	6	300	6	0.1	291
R15N0.25	15	168	6	300	6	0.25	728

04. Residual seismic performance

4.2 Material properties and loading

- Rubber concrete

R (%)	f_{cu} (MPa)				f_c (MPa)
	1	2	3	Average	
0	54.45	54.17	53.02	53.88	42.57
15	42.25	42.16	41.57	41.99	33.17
30	19.67	17.94	16.61	18.07	14.28

- Steel tube and reinforcing bars

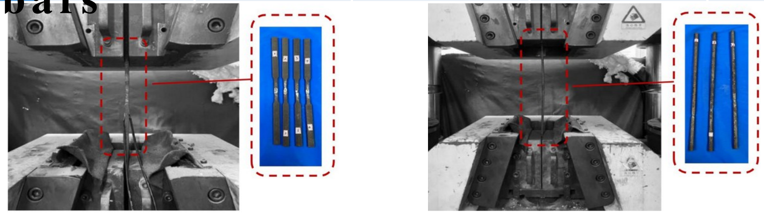

Specimen	t/mm	f_y/MPa	f_u/MPa	Yield ratio
Q355B	6.23	369.79	487.36	0.76
10 mm	10.48	326.63	633.14	0.51
6 mm	6.79	423.92	606.70	0.70

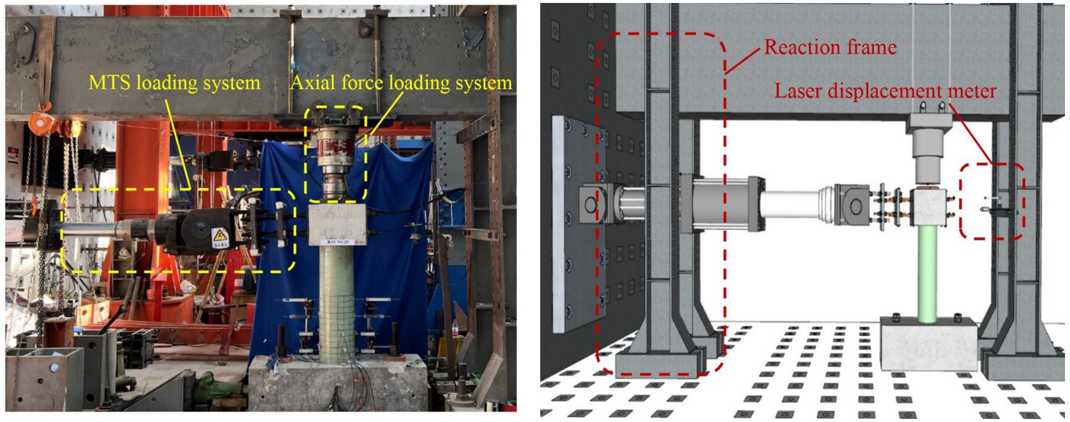

Loading setup

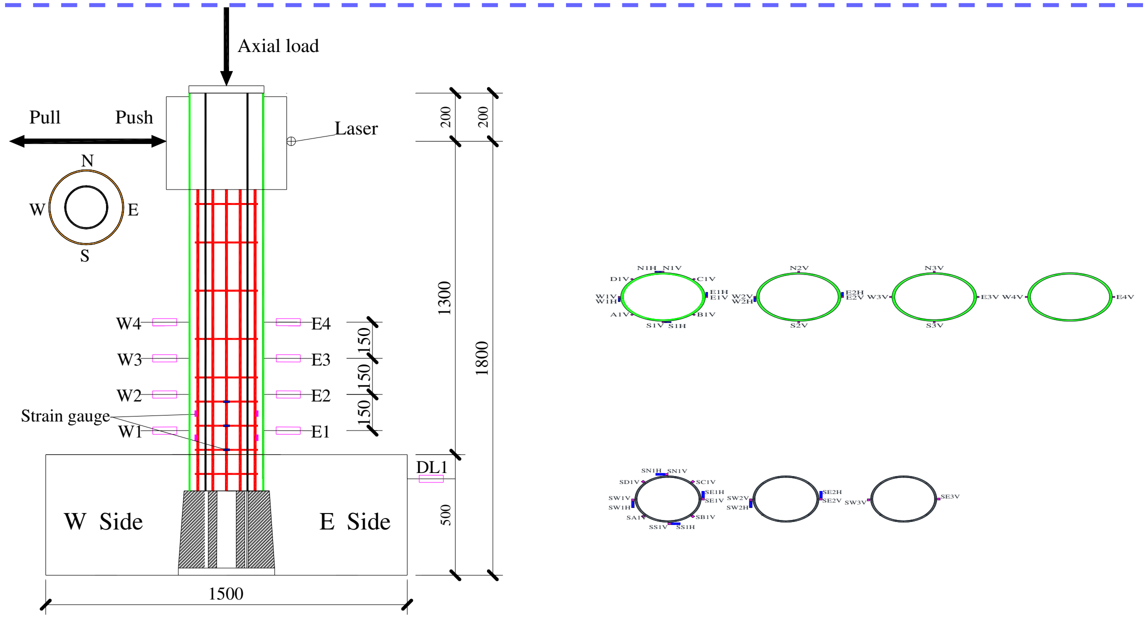

Measurement layout

4.3 Loading scheme and results of the pseudo-dynamic test

Loading protocol

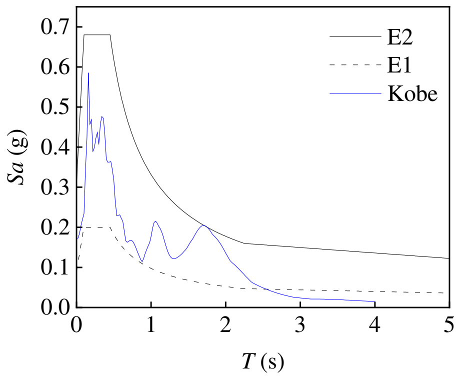

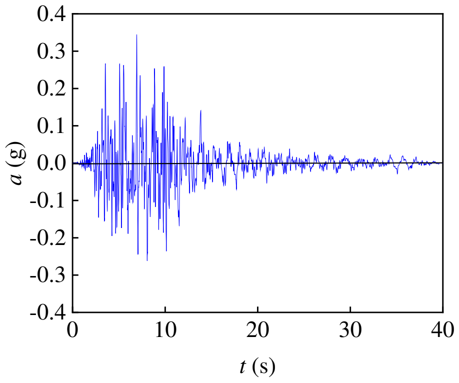

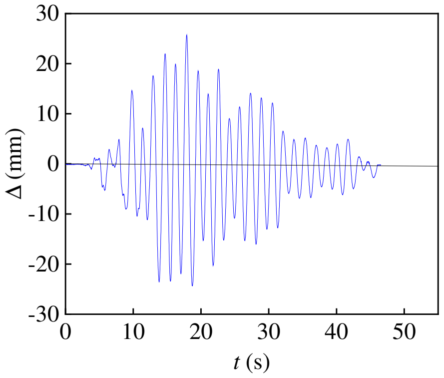

Load-displacement response and failure modes

R0N0.2

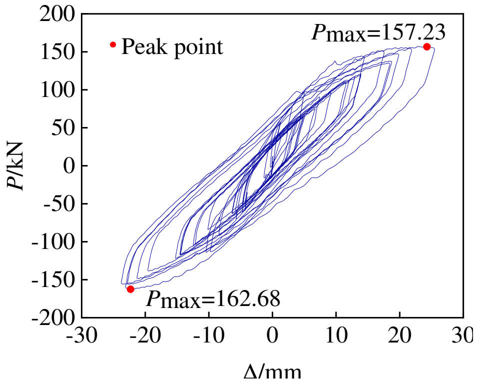

R15N0.2

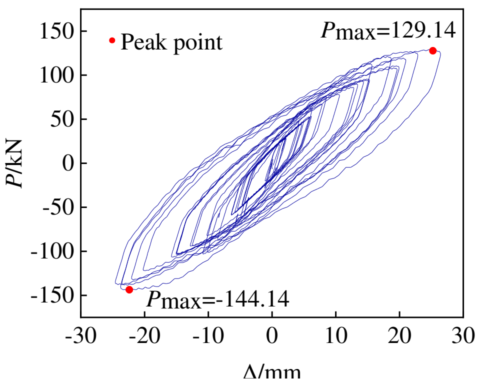

R30N0.2

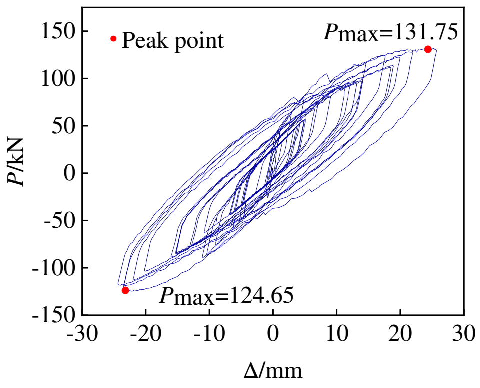

R15N0.1

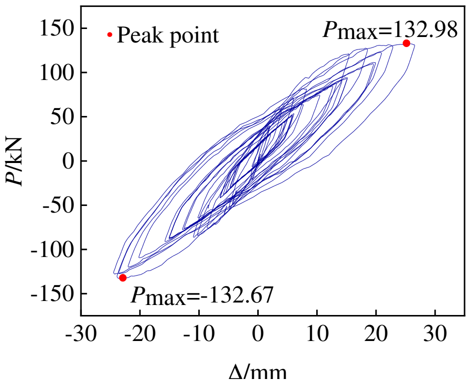

R15N0.2

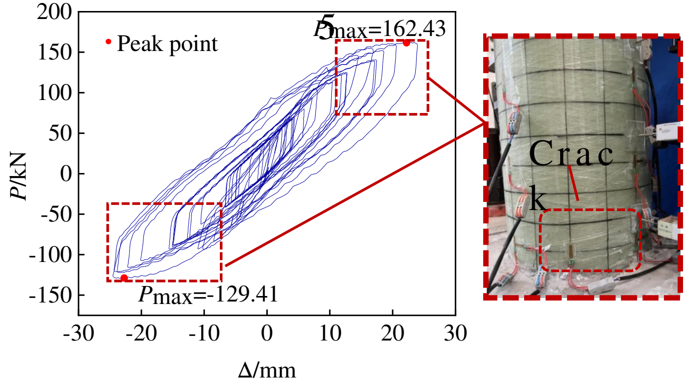

4.4 Loading scheme and results of the quasi-static test

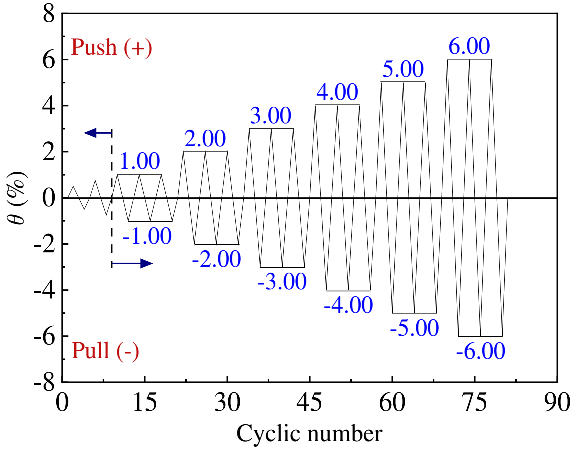

R0N0.2

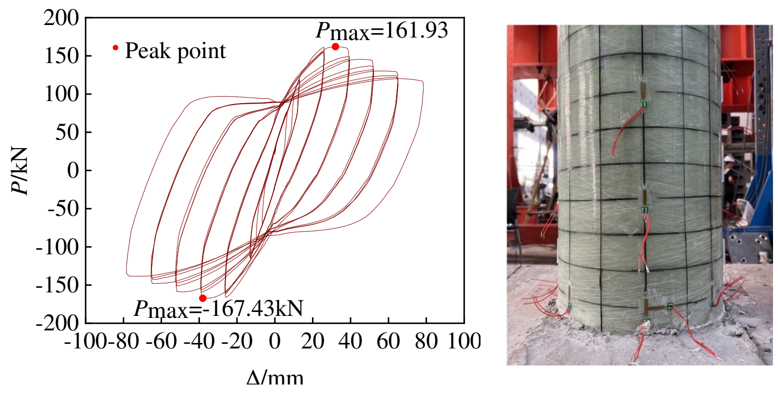

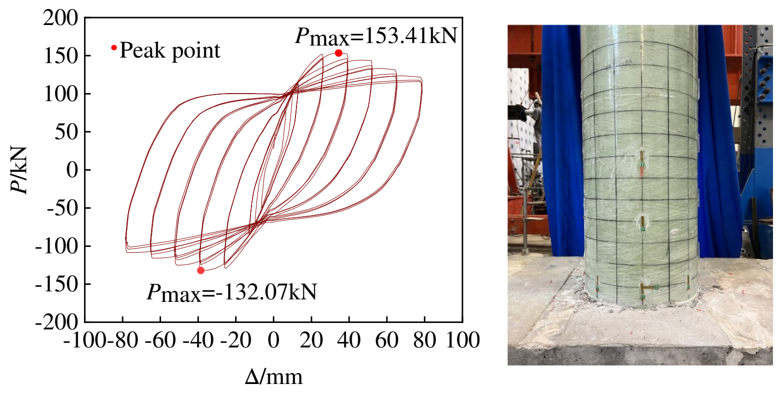

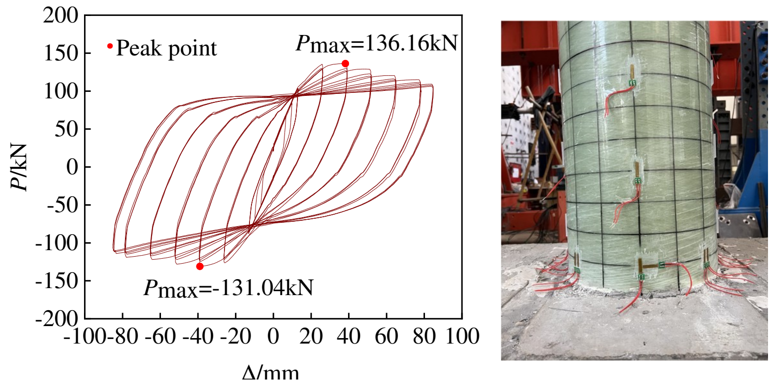

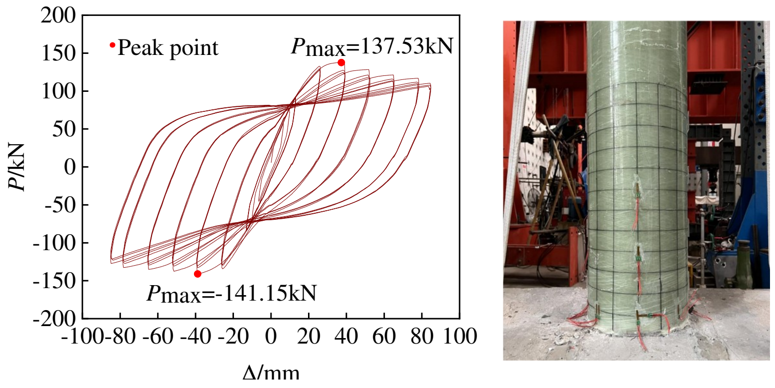

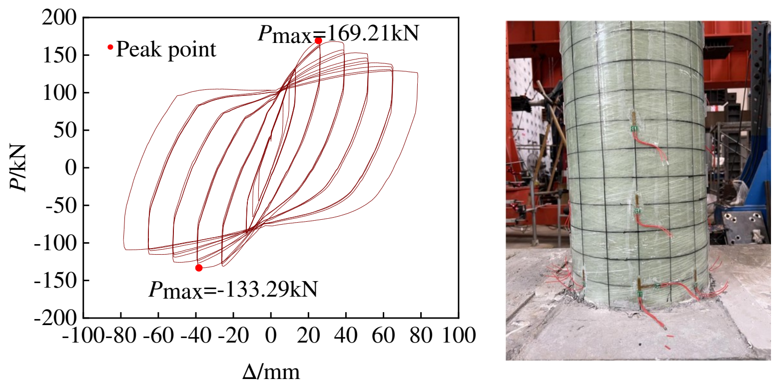

HUAQIAO UNIVERSITY

4.5 Development of skeleton curve models

(1) OY： $\frac{P}{|P^{+}_{max}|}=1.6731\frac{\Delta}{|\Delta^{+}_{max}|}$

(2) YM： $\frac{P}{|P^{+}_{max}|}=0.2769\frac{\Delta}{|\Delta^{+}_{max}|}+0.7126$

(3) MU： $\frac{P}{|P^{+}_{max}|}=-0.1084\frac{\Delta}{|\Delta^{+}_{max}|}+1.0727$

(4) OY⁻： $\frac{P}{|P^{-}_{max}|}=1.6969\frac{\Delta}{|\Delta^{-}_{max}|}$

(5) Y⁻M⁻： $\frac{P}{|P^{-}_{max}|}=0.2571\frac{\Delta}{|\Delta^{-}_{max}|}+0.7443$

(6) M⁻U⁻： $\frac{P}{|P^{-}_{max}|}=-0.1301\frac{\Delta}{|\Delta^{-}_{max}|}+1.1134$

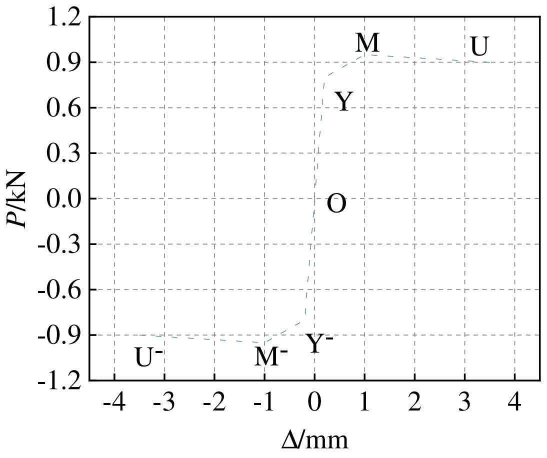

Model of the skeleton curve

R0N0.2

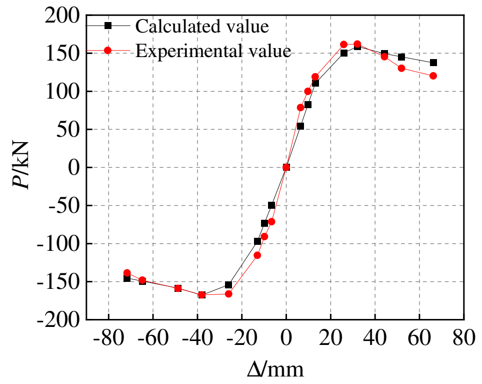

R15N0.2

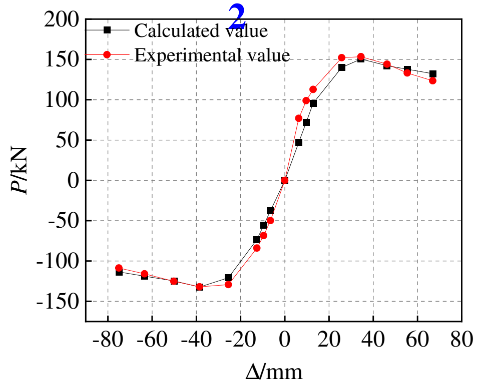

R30N0.2

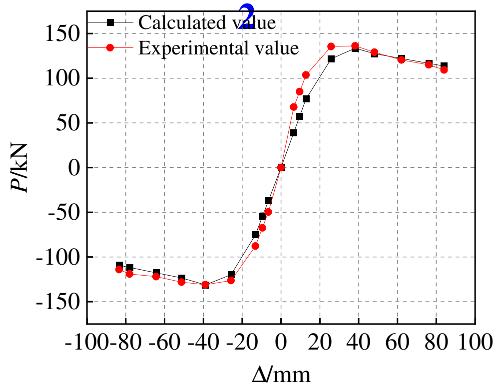

R15N0.1

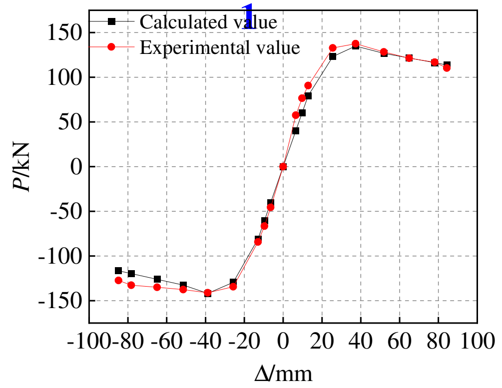

R15N0.25

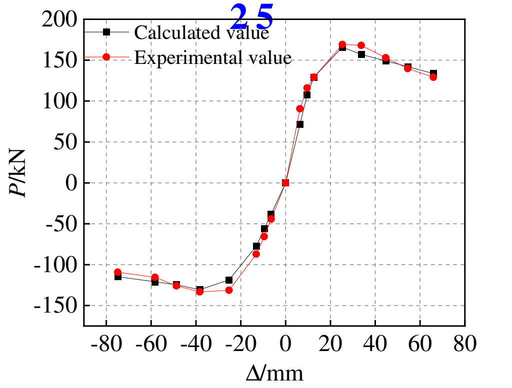

- Ziyang Xie, Xue Han, Jinhuo Zheng, Rong Chen, Zhen Mei, Xiaomei Liu, **Haifeng Li**. Residual seismic behavior of GFRP-rubber concrete-hollow steel tube composite columns[J]. ***Structural Concrete***, 2025, 26(4): 4929-4949.

CONTEN TS

1 Research Background

2 Axial compressive behavior

3 Seismic performance

4 Residual seismic performance

5 Conclusions and Outlook

5.1 Conclusions

- The **configuration** and **cross-sectional forms** of GFRP-steel double-tube confined rubber concrete composite bridge piers are described. The results of **axial compression tests** and **seismic tests** on the composite bridge piers are presented. The **mechanical behavior**, **failure modes**, and **residual seismic performance** of the composite bridge piers are investigated, and the effects of various parameter changes on their behavior are systematically analyzed.
- Based on the plane-section assumption, material constitutive relationships, and mechanical equilibrium equations, a method for determining the **load-carrying capacity** and **seismic design** of GFRP-steel double-tube confined rubber concrete composite bridge piers is proposed.
- The optimized combination of GFRP, rubber concrete, and steel tubes can improve the stress state of the composite structure, thereby enhancing its ductility and deformation capacity and achieving effective vibration reduction and energy

5.2 Outlook

- To investigate the **failure modes**, **energy dissipation capacity**, and **deformation characteristics** of prefabricated composite bridge piers;
- To reveal the effects of key parameters on the **failure mechanisms**, **mechanical behavior**, and **damage evolution** of prefabricated composite bridge piers;
- To establish a refined **finite element model** of prefabricated twin-column bridge piers and extend the parametric analysis of seismic performance in terms of the diameter-to-thickness r… inforcement rati… ther varia…

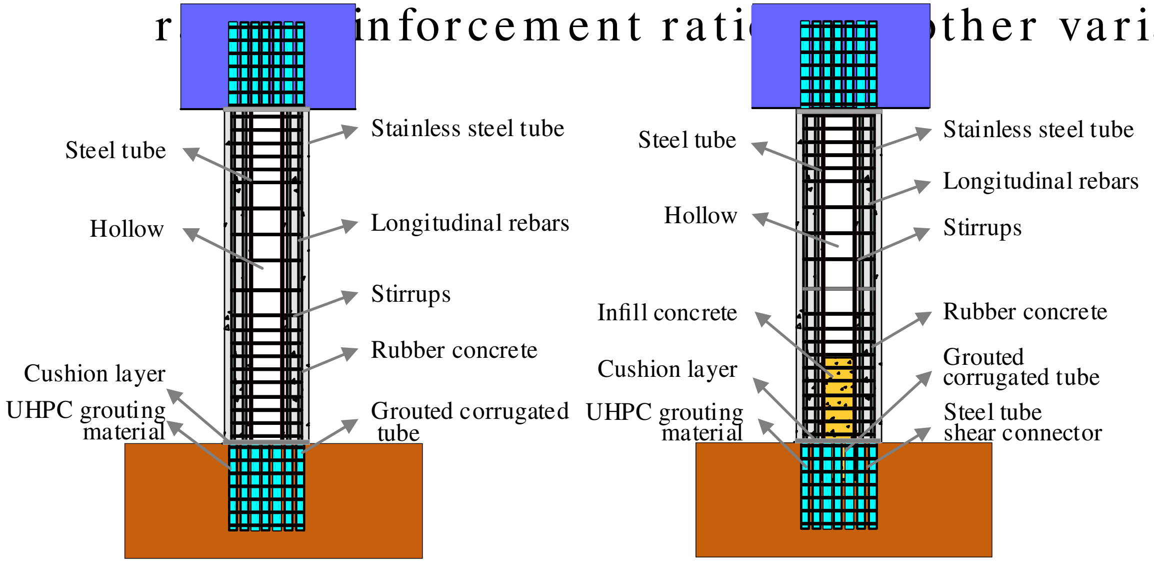

(a) Precast single-column composite piers with double-skin tube confined

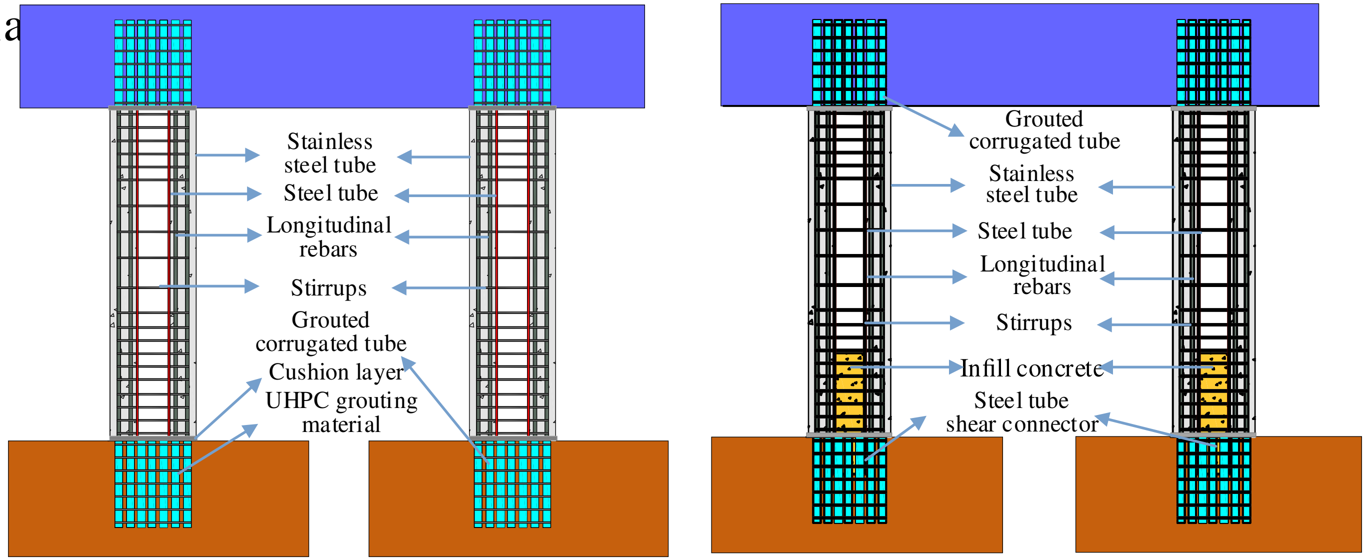

(b) Precast double-column composite piers with double-skin tube confined

5.2 Outlook

- To conduct **quasi-static tests** and **shaking table tests** on prefabricated composite bridge piers with spatial energy-dissipating braces;
- To reveal the **internal force redistribution patterns in the critical regions** of such prefabricated composite bridge piers;
- To propose a **seismic design method** for this type of prefabricated composite

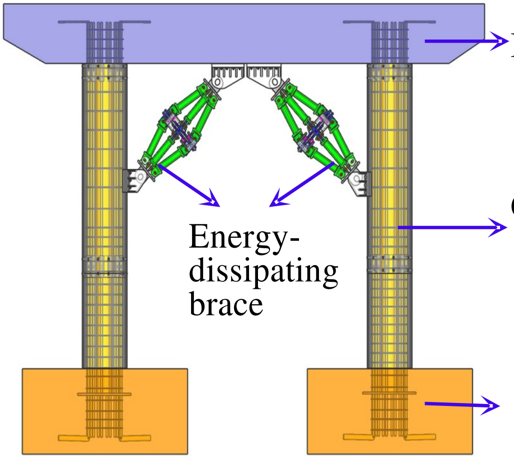

(a) Schematic diagram of

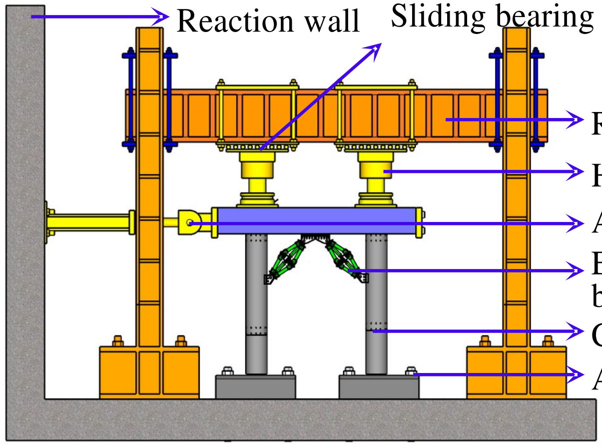

(b) Schematic diagram of quasi-static test for composite

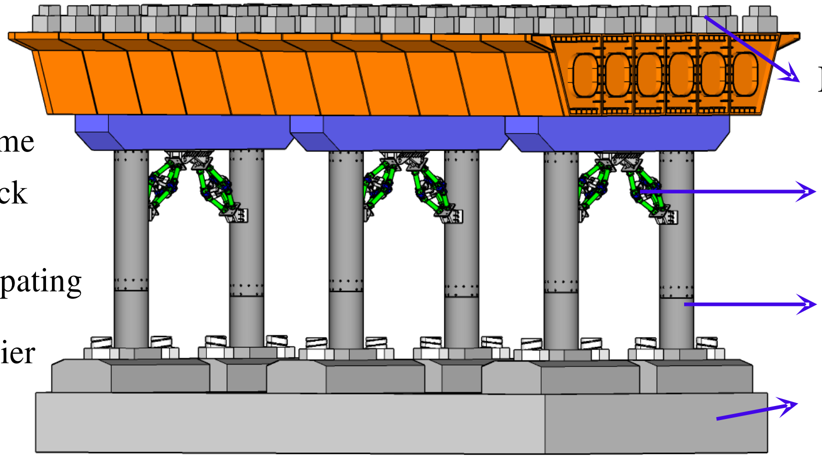

(c) Schematic diagram of shaking table test for composite

06. 实验中心大型设备

■ 大型地震模拟振动台

(1) 台面尺寸： 5 m× 5 m+ 1.5 m × 1.5 m
(2) 控制自由度：三向六自由度
(3) 最大模型质量： 50 T
(4) 满载最大加速度： X/Y:1.5g ; Z:1.0g
(5) 最大倾覆力矩： 150 t•m

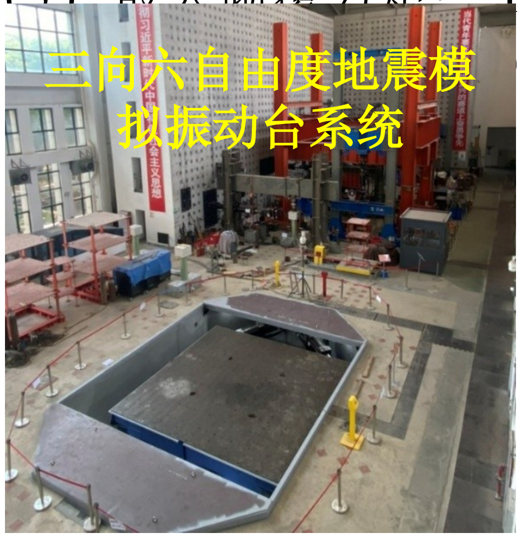

● 大型工程结构火灾实验平台

(1) 包括立式炉、卧式炉、燃烧系统、控制系统、燃气接入
(2) 加载系统和反力系统（ 5000 kN ）
(3) 水平炉膛净尺寸： 6.0 m×4.5 m×1.5 m
(4) 垂直炉膛净尺寸： 4.2 m×2.5 m×3.0

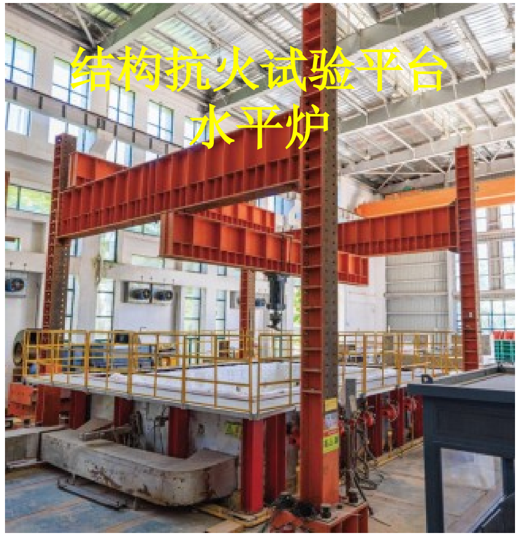

06. 实验中心大型设备

华侨大学 HUAQIAO UNIVERSITY

■ MTS 多通道拟动力试验系统

性能参数

作动器： 14 套 MTS 244 系列

控制器： Flex-Test 100

油源： 505.180 （600LMP）

液压子站： 7 台（190~1500LPM）

● 30000kN 电液伺服多功能结构试验机

性能参数

有效试验力：压≥30000kN

拉≥10000kN

竖向加载净高度：≥5000mm

相邻丝杠净距：≥1700mm

[illegible]底座：长度≥4000mm

宽度≥3200mm

高度≥1100mm

■ MTS 高性能动态疲劳试验机

性能参数

动态荷载能力：优于+/-1000kN

动态行程：不低于 150mm

垂直测试空间：不小于 2500mm

荷载框架立柱间距：不小于 700mm

T 型台深度：不小于 1000mm

● 2000kN 结构疲劳试验机

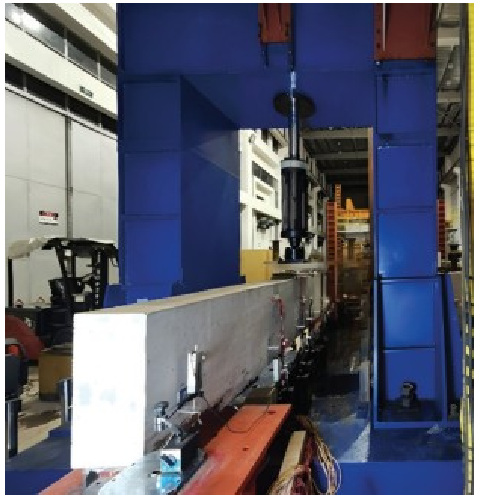

性能参数

试验空间： 1000~3000mm

底座工作区域尺寸： 1500×2000mm

底座外形尺寸： ≥3000×2000mm

试验力： 2000kN

最高工作频率： 20Hz

華僑大學
HUAQIAO UNIVERSITY

Thanks for your attention!

Prof. Hai-feng Li